Available online at www.sciencedirect.com

SCIENCE DIRECT®

Thin Solid Films 469–470 (2004) 268–273

thin solid films

www.elsevier.com/locate/tsf

Thermal reliability of electroless Ni–P–W coating during the aging treatment

Shih-Kang Tien, Jenq-Gong Duh*

Department of Materials Science and Engineering, National Tsing Hua University, 101 Sec. II Kwung-Fu Rd., Hsinchu 300, Taiwan

Available online 27 October 2004

Abstract

The Ni–P–W coating was fabricated by electroless technique in the alkaline solution. The phase transition temperature of Ni–P compound analyzed by differential scanning calorimetry (DSC) was 406 °C. To evaluate the thermal stability of Ni–P–W coating under long-term aging treatment, the operation temperature below and above the crystallization temperature of Ni–P compound was chosen at 375 and 450 °C, respectively. The phase transformation during thermal evolution was studied by X-ray diffraction (XRD). The microstructure and grain size at different stages of aging time were identified by transmission electron microscope (TEM). The surface roughness at as-deposited and final heat treatment states were explored by atomic force microscope (AFM). During the long-term heat treatment at 375 °C, the microhardness firstly increased owing to the crystallization of nickel as well as Ni_3P and then maintained an elevated hardness value. The Ni–P–W coating at 450 °C also exhibited a high elevated-temperature reliability after aging treatment. The hardness of the Ni–P–W coating was substantially increased to 1350 HK for 30 min and reached a maximum hardness of 1460 HK, with grain size of 13 nm for 4 h. However, the strength of the coating was gradually degraded after excessive aging and reached a steady state value around 1200 HK over 20 h, with the grain size pinned around 30 nm.

Keywords: Electroless; Ni–P–W coating; Aging; Reliability; TEM; Thermal evolution

1. Introduction

Hard coating, which exhibits high mechanical strength, corrosion, and wear properties, has been used as a surface modification to protect the substrate and prolong the life span of working piece in many application fields. Especially, the Ni–P coating possesses a distinctive structure and properties, depending on its phosphorus content. The low phosphorus content (1–6 wt.%) of Ni–P coating with a nanocrystalline structure showed good thermal stability and mechanical properties, such as hardness and wear resistance. In addition, the high phosphorus content (9–15 wt.%) of the Ni–P coating with amorphous structure exhibited better corrosion resistance [1–5]. Ni–P coating could be strengthened by suitable annealing due to the precipitation hardening of Ni and Ni_3P. However, for excessive treatment over the precipitation temperature of Ni_3P, the hardness of the binary Ni–P coating would degrade because of the grain coarsening. To enhance the thermal stability of binary Ni–P coating, the ternary Ni–P–Zn [6], Ni–P–Cu [7–9], Ni–P–Cr [10–12], and Ni–P–W [13–19] coatings were proposed that the incorporation of the third element in to the Ni–P-based coating could suppress the precipitation of Ni_3P. It was reported that the ternary Ni–P–W and Ni–P–Cr coatings possessed not only better thermal stability but also high hardness at elevated temperature as compared with the binary coating [10,20,21]. However, the thermal reliability after the long-term aging time in the ternary coating was not yet fully investigated. As a result, this study was mainly focused on the thermal reliability and surface roughness of the ternary electroless Ni–P–W coating at 375 and 450 °C for various aging time. The crystallization behavior of the Ni–P–W coating was identified by X-ray diffraction (XRD). The microstructure and grain size were observed

* Corresponding author. Tel./fax: +886 3 5712686.
E-mail address: jgd@mx.nthu.edu.tw (J.-G. Duh).

0040-6090/$ - see front matter © 2004 Elsevier B.V. All rights reserved.
doi:10.1016/j.tsf.2004.08.179

by transmission electron microscope (TEM). The microhardness tester was used to investigate the strength of the deposit under various conditions. In addition, the surface morphology at the as-deposited and long-term treatment states was detected by atomic force microscope (AFM).

2. Experimental procedure

The electroless Ni–P–W coating was deposited on the mild steel substrate with 15 mm in diameter and 5 mm in thickness. Before deposition, the mild steel was first ground with SiC from #240 to #2400 and polished with diamond slurry to 1 μm. The bath composition for electroless deposition was as followed: (a) sodium sulfate, $Ni_2SO_4 \cdot 6H_2O$ (0.1 M), (b) sodium citrate, $Na_3C_6H_5O_7 \cdot 2H_2O$ (0.35 M), (c) sodium hypophosphite, $NaH_2PO_2 \cdot H_2O$ (0.1 M), (d) sodium tungstate, $Na_2WO_4 \cdot 2H_2O$ (0.1 M). The temperature was maintained at 90±2 °C, and the pH value of the solution adjusted by NaOH was controlled at 9. The sample loaded was 120 cm^2/l. The heat treatment of the deposit was performed isothermally at 375 and 450 °C for different aging time in the N_2-purged atmosphere. The heating rate was all fixed at 10 °C/min.

The composition and the thickness of the Ni–P–W coating were analyzed with an electron probe microanalyzer (JXA-8800, JEOL, Japan). The phase identification of as-deposited and heat-treatment Ni–P–W films were investigated by X-ray diffractometer (Rigaku, Dmmax-B, Tokyo, Japan), using $Cu_{k\alpha}$ radiation with a wavelength of 0.15406 nm generated from a Cu target at 30 keV and 20 mA. The θ–2θ scan range was from 35° to 55° with a step width of 0.02° at a fixed time of 1 s/step. Transmission electron microscopy (JSM-2010, JOEL, Japan) was operated at 200 kV to observe the microstructure and grain size of the Ni–P–W coating under various heat treatment conditions. For the TEM analysis, the film was first ground and polished and then glued onto a Cu grid with 3 mm in diameter. A Gatan dual ion mill with incident angle of 10–15°, 5 keV, and rotation was utilized for the electron transparency. The hardness of as-deposited and heated treatment coating was evaluated with a microhardness tester (MHT-4, Antor Parr, Austria). The load used in the test was 10 g, and the loading time was 15 s. The load was appropriately chosen to avoid the substrate and surface effects. The surface morphology and surface roughness were detected by atomic force microscope (AFM, DI3100, Digital Instrument, USA).

3. Results and discussion

3.1. Thermal reliability

The thickness of the coating observed from the cross-section view was approximately 8 μm. The composition of the Ni–P–W coating analyzed by EPMA was Ni (80.6 wt.%)–P (10.7 wt.%)–W (8.7 wt.%). Long-term aging treatment was used to evaluate the thermal reliability and

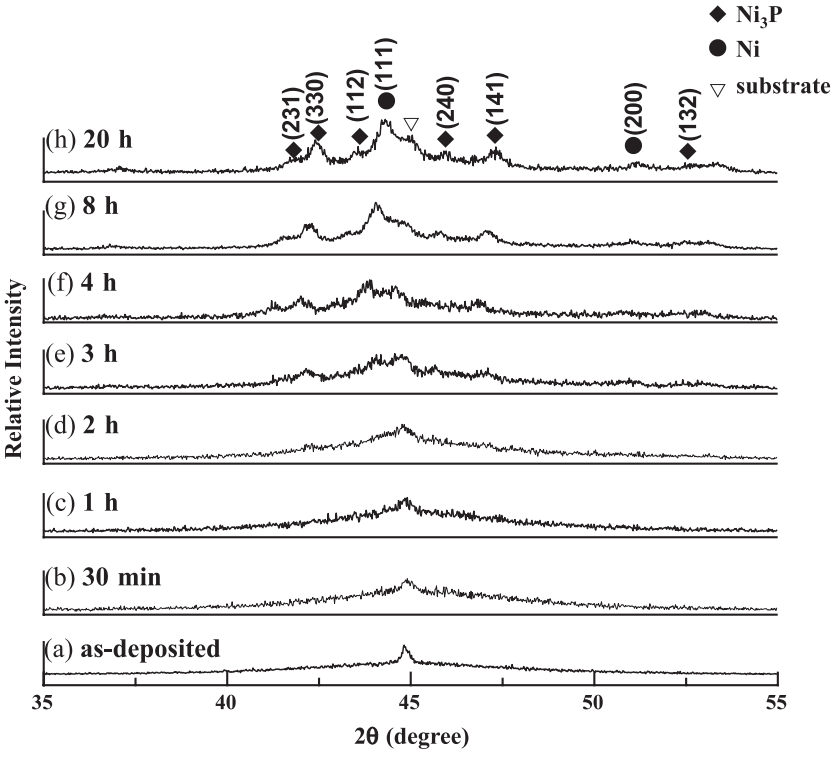

Fig. 1. XRD diffraction patterns of the Ni–P–W coating at the as-deposited and heat treatment states for various aging time at 375 °C.

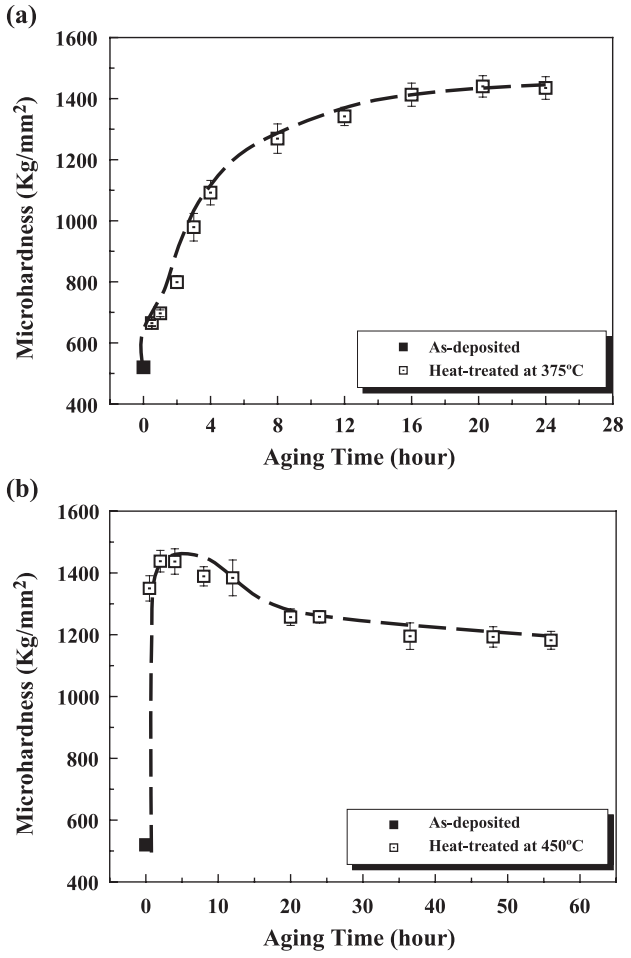

Fig. 2. Hardness of the Ni–P–W coating as a function of aging time at (a) 375 and (b) 450 °C.

surface stability of the electroless Ni–P–W coating for the practical application such as press molding and other high-temperature environment.

3.1.1. Aging test at 375 °C

Fig. 1 presents the X-ray diffraction patterns of the Ni–P–W coating at various heat treatment interval of time at 375 °C. The as-deposited Ni–P–W coating in Fig. 1(a) shows amorphous structure, which comprises a broad peak located around 45° and a sharp peak caused by Fe (111) substrate. Heating at 375 °C for 30 min and 1 h, the diffraction pattern remained unchanged, while the broad peak of Ni (111) became sharper than the as-deposited state. It is suggested that, under the heat treatment (below the crystallization temperature of Ni_3P at 406 °C), the microstructure variation was due to the short-ranged order movement of atoms for annihilation of point defects and the Ni refining [22,23]. The Ni (111) peak was shifted to lower angle and the Ni_3P (231) was formed in amorphous matrix after further treatment at 375 °C for 2 h. The reason that the peak shifted to low angle was the result of the tungsten dissolving into the nickel matrix, which led to the lattice expansion of nickel. For longer heat treatment time at 375 °C for 3 and 4 h, the precipitation of Ni_3P (231), (330), (240), (141), and (132) was observed distinctly in the broadened amorphous matrix. Afterwards, no other peak was formed, while the broadened amorphous matrix gradually disappeared, and the Ni and Ni_3P peaks became sharper instead.

Fig. 2(a) exhibits the relationship between hardness and aging time at 375 °C. The variation of hardness could be correlated with the XRD results in Fig. 1. The hardness of the as-deposited Ni–P–W coating was 520 HK, which was

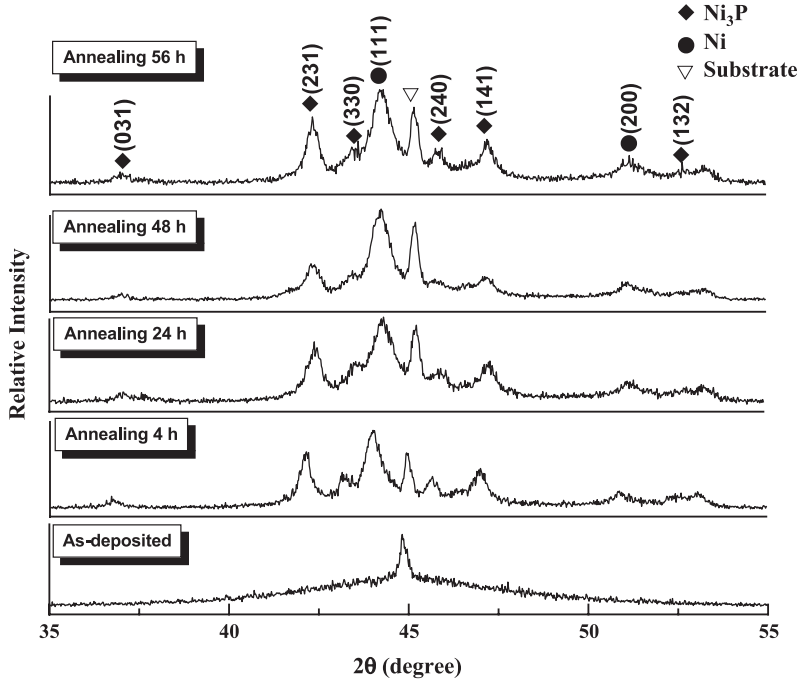

Fig. 3. XRD diffraction patterns of the Ni–P–W coating at the as-deposited and heat treatment states for various aging time at 450 °C.

relatively low due to the amorphous structure. Heating at 375 °C for 30 min and 1 h, the hardness of the deposit was slightly increased to 667 and 697 HK, respectively, which was caused by the precipitation of Ni in the amorphous matrix. When heating at 375 °C for 2 h, the hardness was increased up to 799 HK, owing to the solution hardening of tungsten into the nickel matrix and the partial precipitation of Ni_3P in the Ni–P–W coating. Moreover, the strength of Ni–P–W deposit was rapidly enhanced from 2 to 3 h at 375 °C. The obvious increase in hardness was mainly resulted from the precipitation hardening of Ni_3P in the amorphous matrix. After further aging at 375 °C for 3 h, the hardness increased slowly. The hardness variation over 3 h was attributed to the transformation of amorphous structure into the crystalline phases, which led to the disappearance of broadened peak and the grain growth of Ni and Ni_3P, as can be observed in Fig. 1. Finally, the hardness reached a steady state value after 20 h. The shape and intensity of XRD peaks remained identical, indicating that the grain size of Ni and Ni_3P was pinned and unchanged [24].

3.1.2. Aging test at 450 °C

Fig. 2(b) illustrates the hardness as a function of aging time at 450 °C (higher than the crystallization temperature of Ni_3P). For the thermal treatment at 450 °C for 30 min, the hardness of the Ni–P–W coating was abruptly increased from 520 to 1350 HK and then reached a maximum value of 1460 HK at 450 °C for 4 h. After further heating, the strength of the coating was slightly decreased to around 1200 HK and maintained a steady state value.

In Fig. 3, the amorphous structure of as-deposited Ni–P–W coating was transformed into the crystalline Ni and Ni_3P phases. The precipitation hardening of Ni and Ni_3P led to the rapid increase in hardness. After further heating at 450 °C,

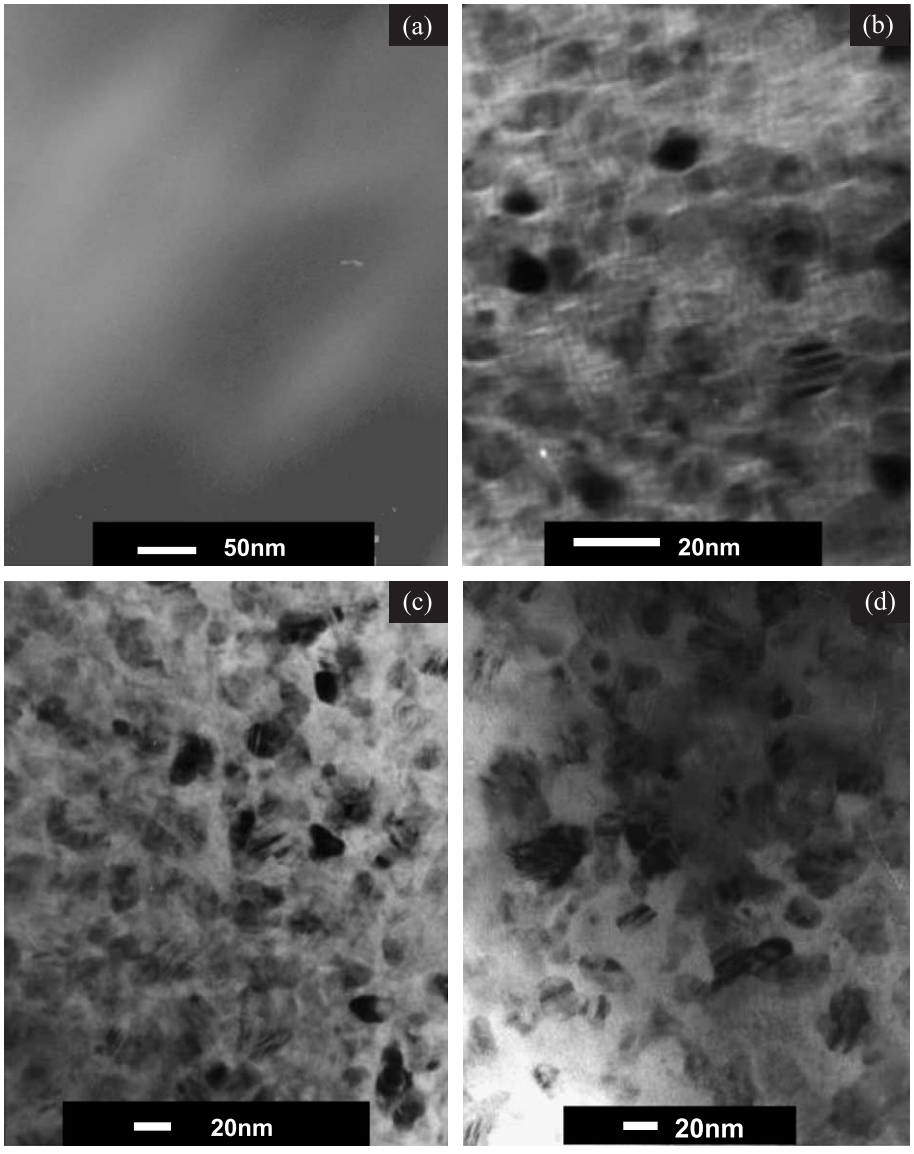

Fig. 4. TEM micrographs of the Ni–P–W coating under various states: (a) as-deposited, (b) 450 °C for 4 h, (c) 450 °C for 24 h, and (d) 450 °C for 56 h.

XRD patterns of Ni–P–W coating remained unchanged even for 56 h. It is reported that the binary Ni–P coating with the maximum hardness of approximately 1200 HK at 350 °C for 4 h exhibited a poor thermal stability and hardness at 450 °C [21]. The hardness of Ni–P coating after thermal treatment at 450 °C for 30 min was decreased to 1000 HK. Moreover, after excessive aging at 450 °C for 4 h, the mechanical property of binary Ni–P deposit was further decreased to lower value compared with its maximum hardness. However, the ternary Ni–P–W coating with the addition of tungsten could maintain a high value for 56 h, which was comparable to the maximum hardness in the binary Ni–P coating at 350 °C for 4 h. As a result, the coplating of tungsten into the binary Ni–P coating could achieve a significant improvement in the thermal reliability application and prolong the life span at heat-treatment environment.

Fig. 4 displays the bright-field image of the Ni–P–W coating after the heat treatment at 450 °C for various time. The as-deposited Ni–P–W coating observed in Fig. 4(a) shows amorphous structure, which is consistent with the result of XRD. From the analysis of XRD, the diffraction patterns at 450 °C for 4 , 24, and 56 h were similar and indistinguishable. Nevertheless, the detailed microstructure evolution could be investigated by TEM. The grain size of the Ni–P–W coating at different heat treatment conditions is listed in Table 1. The grain size of the Ni–P–W coating at 450 °C for 4 h, which exhibited the maximum hardness in Fig. 2(b), was 13.6 nm. After further heating over 20 h, the hardness was decreased to 1200 HK and remained nearly unchanged afterwards. As observed from the TEM micrograph in Fig. 4(c) and (d), the grain size of the Ni–P–W coating at 450 °C for 24 h grew up to 31 nm, while that of the Ni–P–W coating over 24 h was still pinned around 34 nm. It appears that the heat applied in the Ni–P–W coating at 450 °C over 20 h could not provide sufficient energy to render the grain growth. The degradation in hardness did not occur due to the suppression of grain coarsening. Therefore, the hardness of the Ni–P–W coating after heat treatment at 450 °C over 20 h maintained at high strength of 1200 HK. Zhang at al. proposed that the grain size of binary Ni–P coating after long-term heat treatment at 300, 350, and 400 °C could reach equilibrium whether the operation temperature was below the crystallization temperature of Ni_3P compound [24]. The higher the temperature, the larger the equilibrium grain size is. Furthermore, the hardness at various conditions after long-term treatment could also reach equilibrium strength due to the grain boundary pinning [24].

Table 1
Grain size and hardness of the Ni–P–W coating at the as-deposited and heat treatment states

Sample	Grain size (nm)	Hardness (HK)
As-deposited	–	520±17
450, 4 h	13.6±1.6	1460±41
450, 24 h	31.5±3.3	1258±20
450, 56 h	34.3±4.3	1182±29

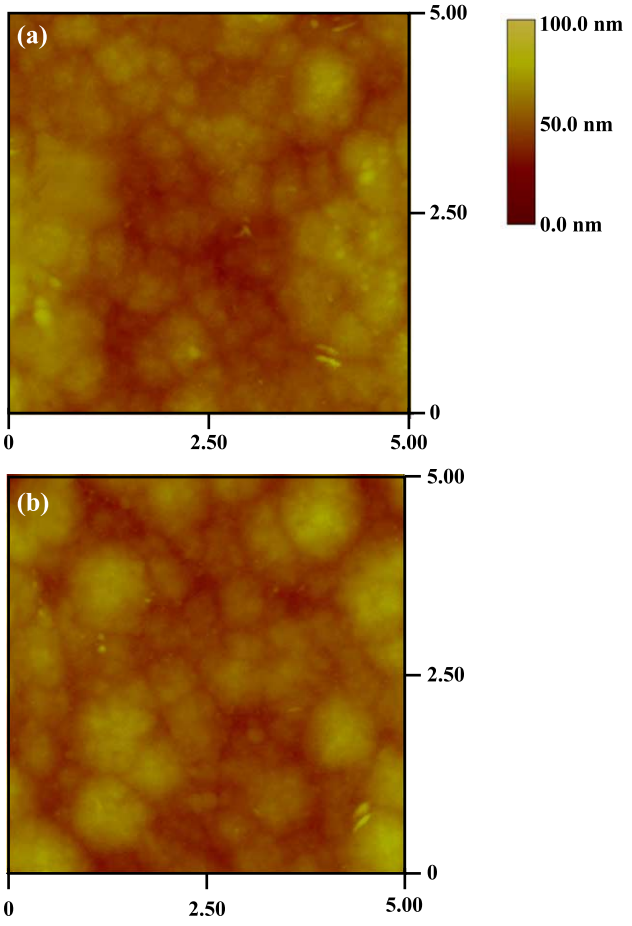

Fig. 5. AFM images of electroless Ni–P–W coating at (a) as-deposited state and at (b) 450 °C for 56 h.

It is believed that the addition of tungsten into the Ni–P-based coating could enhance the thermal reliability and hardness after long-term heat treatment at 375 and 450 °C, as compared to the binary Ni–P coating.

3.2. Surface morphology

Fig. 5 exhibits the surface morphology of the Ni–P–W coating at as-deposited and 450 °C for 56 h investigated by atomic force microscope with the scan area of 5×5 μm^2. The as-deposited coating showed that the nodule-like morphology and the surface roughness was 6.5 nm in Ra. Heating at 450 °C for 56 h, the surface morphology remained unchanged, and the surface roughness was slightly increased to 9.3 nm in Fig. 5(b). It is apparent that the surface roughness remained unaltered after the long-term heat treatment at 450 °C.

4. Conclusions

The electroless Ni–P–W coating at 375 °C, which was below the crystallization temperature of Ni_3P, was strengthened up to 1440 HK by the crystallization of Ni, solution

hardening of tungsten into the nickel matrix, the precipitation of Ni_3P, and then the hardness of the coating maintained unchanged even after 20-h heat treatment. On the other hand, when heated at 450 °C, which was above the crystallization temperature of Ni_3P, the hardness of the Ni–P–W coating was substantially increased to 1350 HK for 30 min and reached a maximum hardness of 1460 HK, with grain size of 13 nm for 4 h. The strength of the coating was then gradually degraded after excessive aging and reached a steady state value around 1200 HK over 20 h. The grain size at 450 °C for 24 and 56 h remained around 30 nm. The hardness of the Ni–P–W with the addition of tungsten after long-term heat treatment at 450 °C could still maintain 1200 HK, which was comparable to the maximum hardness of binary Ni–P coating and was much superior than that of Ni–P coating after the heat treatment at 450 °C. In addition, the surface morphology of the Ni–P–W coating after the long-term treatment at 450 °C for 56 h was rather uniform, similar to that at the as-deposited state. It is concluded that the electroless Ni–P–W coating in this study exhibited high thermal reliability after long-term aging test at both 375 and at 450 °C.

Acknowledgement

This work was supported by the National Science Council under contract No. NSC 92-2216-E-007-036.

References

[1] I. Apachitei, F.D. Tichelaar, J. Duszczyk, L. Katgerman, Surf. Coat. Technol. 149 (2002) 263.
[2] K.H. Hur, J.-H. Jeong, D.N. Lee, J. Mater. Sci. 25 (1990) 2573.
[3] H. Kreye, F. Muller, K. Lang, D. Isheim, T. Hentschel, Z. Metallkd. 86 (1995) 184.
[4] R.N. Duncan, Plat. Surf. Finish. 83 (1996) 65.
[5] I. Apachitei, J. Duszczyk, Surf. Coat. Technol. 132 (2000) 89.
[6] M. Schlesinger, X. Meng, D.D. Snyder, J. Electrochem. Soc. 137 (1990 June) 1858.
[7] Y.C. Chang, J.G. Duh, Y.I. Chen, Surf. Coat. Technol. 139 (2001) 233.
[8] C.J. Chen, K.L. Lin, J. Electrochem. Soc. 146 (1) (1999) 137.
[9] S. Armyanov, J. Georgieva, D. Tachev, E. Valova, N. Nyagolova, S. Mehta, D. Leibman, A. Ruffini, Electrochem. Solid-State Lett. 2 (7) (1999) 323.
[10] W.Y. Chen, J.G. Duh, Surf. Coat. Technol. 177–178 (2004) 222.
[11] C.F. Conde, H. Miranda, A. Conde, R. Marquez, J. Mater. Sci. 24 (1989) 139.
[12] K. Maeda, T. Ikari, Y. Akashi, K. Futagami, J. Mater. Sci. 29 (1994) 1449.
[13] Y.Y. Tsai, F.B. Wu, Y.I. Chen, P.J. Peng, J.G. Duh, S.Y. Tsai, Surf. Coat. Technol. 146–147 (2001) 502.
[14] B.W. Zhang, W.Y. Hu, Q.L. Zhang, X.Y. Qu, Mater. Charact. 37 (1996) 119.
[15] B.W. Zhang, W.Y. Hu, X.Y. Qu, Q.L. Zhang, H. Zhang, Z.S. Tan, Trans. IMF 74 (2) (1996) 69.
[16] T. Osaka, H. Sawai, F. Otoi, K. Nihei, Metal Finish. 80 (1982) 31.
[17] K. Aoki, O. Takano, Plat. Surf. Finish. 3 (1990) 48.
[18] I. Koiwa, M. Usuda, T. Osaka, J. Electrochem. Soc. 135 (5) (1988) 1222.
[19] E. Valova, S. Armyanov, A. Franquet, A. Hubin, O. Steenhaut, J.-.L. Delplancke, J. Vereecken, J. Appl. Electrochem. 31 (2001) 1367.
[20] F.B. Wu, Y.I. Chen, P.J. Peng, Y.Y. Tsai, J.G. Duh, Surf. Coat. Technol. 150 (2002) 232.
[21] S.K. Tien, J.G. Duh, Surf. Coat. Technol. 177–178 (2004) 532.
[22] T. Hentschel, D. Isheim, R. Kirchheim, F. Muller, H. Kreye, Acta Mater. 48 (2000) 933.
[23] I. Apachitei, F.D. Tichelaar, J. Duszczyk, L. Katgerman, Surf. Coat. Technol. 148 (2001) 284.
[24] Y.Z. Zhang, Y.Y. Wu, M. Yao, J. Mater. Sci. Lett. 17 (1998) 37.